Available online at www.sciencedirect.com
SCIENCE DIRECT®
Icarus 165 (2003) 391–406
ICARUS
www.elsevier.com/locate/icarus

Methane in Oort cloud comets

E.L. Gibb,[a,*] M.J. Mumma,[b] N. Dello Russo,[b,c] M.A. DiSanti,[b] and K. Magee-Sauer[d]

[a] *NAS-NRC, Laboratory for Extraterrestrial Physics, NASA Goddard Space Flight Center Code 690, Greenbelt, MD 20771, USA*
[b] *Laboratory for Extraterrestrial Physics, NASA Goddard Space Flight Center Code 690, Greenbelt, MD 20771, USA*
[c] *Department of Physics, The Catholic University of America, Washington, DC 20064, USA*
[d] *Department of Chemistry and Physics, Rowan University, Glassboro, NJ 08028, USA*

Received 17 December 2002; revised 18 June 2003

Abstract

We detected CH_4 in eight Oort cloud comets using high-dispersion ($\lambda/\Delta\lambda \sim 2 \times 10^4$) infrared spectra acquired with CSHELL at NASA's IRTF and NIRSPEC at the W.M. Keck Observatory. The observed comets were C/1995 O1 (Hale–Bopp), C/1996 B2 (Hyakutake), C/1999 H1 (Lee), C/1999 T1 (McNaught–Hartley), C/1999 S4 (LINEAR), C/2000 WM_1 (LINEAR), C/2001 A2 (LINEAR), and 153/P Ikeya–Zhang (C/2002 C1). We detected the R0 and R1 lines of the ν_3 vibrational band of CH_4 near 3.3 μm in each comet, with the exception of McNaught–Hartley where only the R0 line was measured. In order to obtain production rates, a fluorescence model has been developed for this band of CH_4. We report g-factors for the R0 and R1 transitions at several rotational temperatures typically found in comet comae and relevant to our observations. Using g-factors appropriate to T_{rot} as determined from HCN, CO and/or H_2O and C_2H_6, CH_4 production rates and mixing ratios are presented. Abundances of CH_4/H_2O are compared among our existing sample of comets, in the context of establishing their place of origin. In addition, CH_4 is compared to native CO, another hypervolatile species, and no correlation is found among the comets observed.

Keywords: Comets, composition; Infrared observations; Spectroscopy

1. Introduction

Methane is an important constituent of interstellar and cometary volatile composition. However, since CH_4 is a symmetric hydrocarbon without a permanent dipole moment, the only observable transitions for gas phase emission in cometary comae are the ro-vibrational bands in the infrared spectral region. Attempts to detect fluorescent emission in the ν_3 band of methane near 3.3 μm were first made in comets C/1973 E1 (Kohoutek) and 1P/Halley (Roche et al., 1975; Kawara et al., 1988; Drapatz et al., 1987). A marginal detection of CH_4 was claimed in Comet Wilson (1986I) (Larson et al., 1989) and an upper limit of 0.31 percent relative to water was reported for Comet C/Levy (1990 c) (Brooke et al., 1991).

Cometary CH_4 was first unambiguously detected in ground-based observations of C/1996 B2 (Hyakutake) (Mumma et al., 1996). Since then, firm detections of the R0 and R1 lines have been made in several comets, including C/1995 O1 (Hale–Bopp), C/1999 S4 (LINEAR), C/2001 A2 (LINEAR), C/2000 WM_1 (LINEAR), C/1999 H1 (Lee), and most recently 153/P Ikeya–Zhang (C/2002 C1). In addition, the R0 line was observed in C/1999 T1 (McNaught–Hartley) and the P2 and P3 lines were observed in Hyakutake (we do not report values for P3 since it is blended with CH_3OH).

In Section 2 we discuss the observations and data analysis. We present the CH_4 ν_3 band fluorescence model and resulting g-factors in Section 3. In Section 4 we present production rates and mixing ratios for CH_4, and discuss some possible implications and scenarios in Section 5. We summarize our results in Section 6.

2. Observing approach and data reduction

Observations were performed using the long-slit spectrometers CSHELL at NASA's 3-meter IRTF and NIRSPEC at the 10-meter W.M. Keck Observatory, both located at Mauna Kea, Hawaii. Both instruments are high-dispersion cryogenic echelle spectrometers with sensitivity in the 1–5.5 μm spectral region. For the CSHELL observations of

* Corresponding author.
E-mail address: egibb@nd.edu (E.L. Gibb).

0019-1035/$ – see front matter
doi:10.1016/S0019-1035(03)00201-X

Table 1
Observations

Comet	Date	Transition (ν_3)	$R_\odot$ (AU)	Δ (AU)	Δ-dot (km/s)	t_{int} (s)	Slit width (arcsec)	Instrument
C/1996 B2 (Hyakutake)	24.4 March 1996	R0	1.060	0.106	−15.5	240	1	CSHELL
		R1				240	1	CSHELL
	10.2 April 1996	P2	0.685	0.533	56.2	240	1	CSHELL
	12.2 April 1996	R0	0.638	0.596	56.5	240	1	CSHELL
		R1				120	1	CSHELL
		P2				120	1	CSHELL
C/1995 O1 (Hale–Bopp)	24.2 February 1997	R0	1.114	1.568	−28.8	120	1	CSHELL
	30.0 April 1997	R0	1.048	1.753	29.6	240	1	CSHELL
		R1				120	1	CSHELL
	1.0 May 1997	R0	1.056	1.770	29.6	120	1	CSHELL
C/1999 H1 (Lee)	19.6 August 1999	R0 + R1	1.049	1.381	−28.4	480	0.432	NIRSPEC
	21.6 August 1999	R0 + R1	1.076	1.348	−29.0	1560	0.432	NIRSPEC
C/1999 S4	13.6 July 2000	R0 + R1	0.810	0.578	−56.7	1680	0.742	NIRSPEC
C/1999 T1 (McNaught–Hartley)	4.7 March 2001	R0	1.710	1.450	18.1	3600	2	CSHELL
C/2001 A2	9.5 July 2001	R0 + R1	1.161	0.276	11.5	1680	0.432	NIRSPEC
	10.5 July 2001	R0 + R1	1.173	0.282	12.4	2400	0.432	NIRSPEC
C/2000 WM_1	23.3 November 2001	R0 + R1	1.355	0.383	−23.7	3120	0.432	NIRSPEC
153/P Ikeya–Zhang (C/2002 C1)	21.9 March 2002	R0	0.512	0.761	−31.8	960	1	CSHELL
		R1	0.516	0.742		480	1	CSHELL
	22.9 March 2002	R1	0.733	0.490	−31.2	960	1	CSHELL

Hyakutake, Hale–Bopp, and Ikeya–Zhang, a 1-arcsec (5-pixel) wide slit was used while a 2-arcsec wide slit was used for observations of McNaught–Hartley. These slits provide spectral resolving powers $\lambda/\Delta\lambda \sim 25000$ and 15000, respectively. A 3-pixel (0.43-arcsec) wide slit was used with NIRSPEC for comets Lee, A2, and WM_1 ($\lambda/\Delta\lambda \sim 25000$). For S4, a 5-pixel (0.72-arcsec) wide slit was used with NIRSPEC ($\lambda/\Delta\lambda \sim 15000$). The small pixel sizes (0.2×0.2-arcsec for CSHELL and 0.14×0.19-arcsec for NIRSPEC) provide seeing-limited angular resolution along the slit. A summary of the observations is given in Table 1. Flux calibrations were based on observations of standard stars through a wider slit (4-arcsec) using CSHELL. For NIRSPEC observations, the 3- and 5-pixel slits were used, and a slit-loss correction was included in our analysis.

Observations were taken in an observing sequence ABBA, nodding either on or off the chip. For nodding off-chip, A observations placed the comet at the slit center, and B sampled blank sky 2-arcmin perpendicular to the slit length (N or S). For nodding on-chip, A and B were taken in positions approximately one-quarter of the distance from the top and bottom of the slit, respectively. This increased the signal-to-noise by as much as $\sqrt{2}$ for an observation by doubling the time on source per second of clock time. However, this mode of observation limits the spatial coverage along the slit compared with nodding off-chip.

Data were processed using algorithms specifically tailored to our comet observations and include dark subtraction, flat fielding, and removal of cosmic ray hits. Detailed descriptions of our observing procedures and data processing techniques have been discussed elsewhere (Dello Russo et al., 1998, 2000, 2001; Magee-Sauer et al., 1999; DiSanti et al., 2001).

Atmospheric models were obtained using the Spectral Synthesis Program (SSP, Kunde and Maguire, 1974), which uses the HITRAN 1992 Molecular Data Base (Rothman et al., 1998). We used these SSP models to assign wavelength scales to the extracted spectra and to determine column burdens for the absorbing species in the Earth's atmosphere, primarily water and methane in this study. The atmospheric model is binned to the resolution of the comet spectrum, normalized, and scaled to the comet continuum level.

Figure 1 shows 5-row (1-arcsec) spectral extracts for each observation, centered on the gas emission peak. The dashed line is the atmospheric model fit. The difference between the atmospheric fit and the observed comet spectrum gives the residual cometary emission spectrum, convolved with the atmospheric transmittance function (shown below each spectrum in Fig. 1). Methane emission lines are labeled. The 3-σ uncertainty level at the Doppler-shifted position for CH_4 is indicated on each plot. The deep atmospheric absorption lines are due primarily to water ($2\nu_2$ band) and methane. Cometary OH* (1–0) prompt emission lines (Mumma et al., 2001a), as well as the R1 and R0 lines of CH_4, are clearly seen in emission in NIRSPEC spectra (Fig. 1b).

Production rates (in molecules s^{-1}) are calculated by assuming the idealized case of spherically symmetric outflow at uniform velocity, $v_{gas} = 0.8 R_h^{-0.5}$ km s^{-1}. The only exception to this was the high production rate comet Hale–

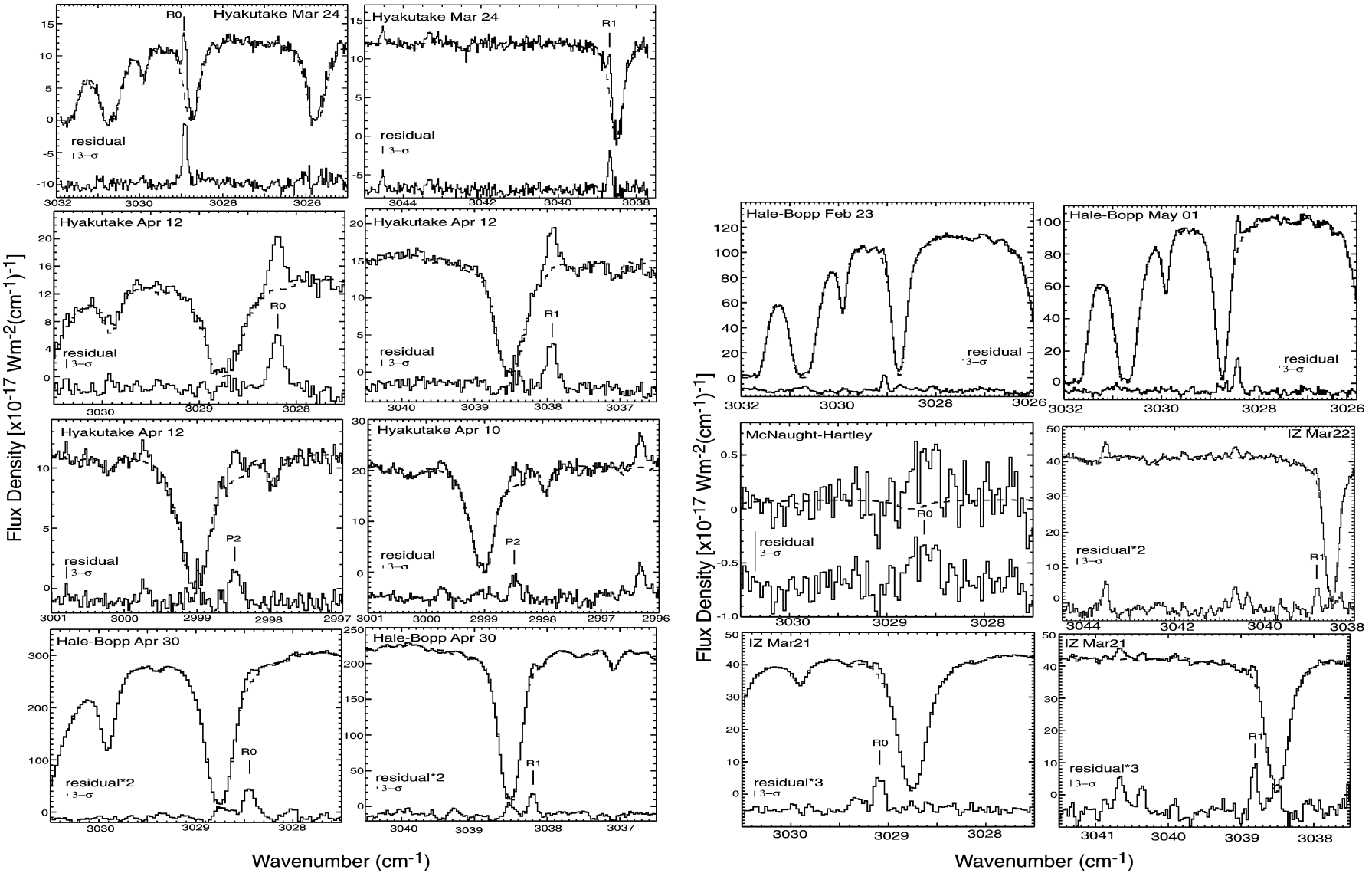

(a)

Fig. 1. Spectra for each comet observed in this study. (a) shows CSHELL spectra of comets Hyakutake, Hale–Bopp, McNaught–Hartley, and Ikeya–Zhang, and (b) shows NIRSPEC (KL2 setting, order 23) spectra of comets Lee, S4, WM_1, and A2. Doppler-shifted positions of the appropriate lines of methane are indicated, as well as the OH^* emissions where applicable. The dashed line is the atmospheric model fit. Underneath the spectra are the residuals determined by subtracting the atmospheric fit from the comet spectrum. The 3-σ uncertainty level at the Doppler-shifted CH_4 position is indicated.

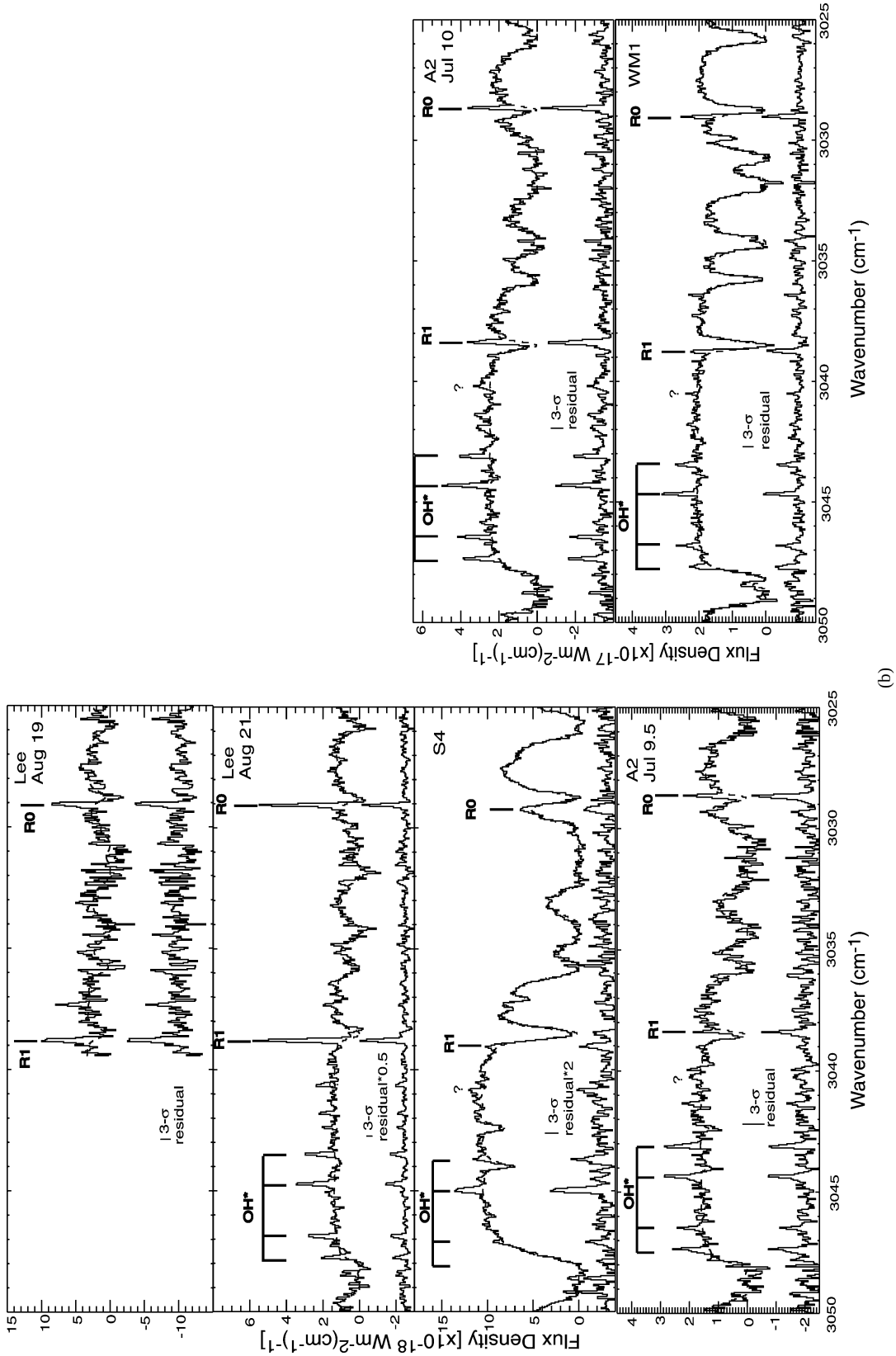

(b)

Fig. 1. Continued.

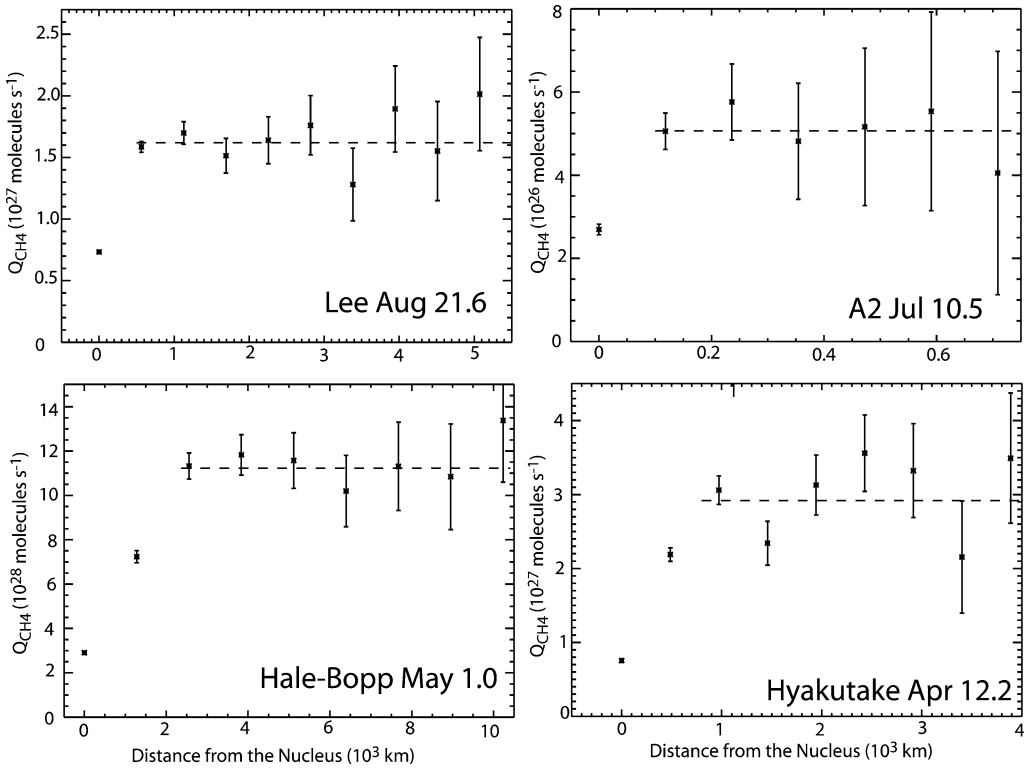

Fig. 2. Sample production rate growth curves (Q-curves) for CH_4 in comets Lee on 21.6 August, A2 on 10.5 July, Hale–Bopp on 1.0 May, and Hyakutake on 12.2 April. The Q-curve was generated by stepping 1×1-arcsec extracts averaged east and west of the nucleus over the range in Table 3. The dashed line is a best fit to the weighted average of these symmetric production rates ($*$), resulting in the global spherical production rates reported in Table 3.

Bopp where radio observations indicate $v_{\rm gas} = 1.1 R_h^{-0.5}$ km s^{-1} (Biver et al., 1999).

A symmetric Q-curve is constructed from the mean emission intensity to either side of the nucleus measured in 1-arcsec intervals along the spatial direction of the slit according to:

$$Q = \frac{4\pi \Delta^2 F_i}{g_i \tau (hc\nu) f(x)}, \quad (1)$$

(see Dello Russo et al., 1998, 2000, Magee-Sauer et al., 1999; and DiSanti et al., 2001 for more details). Here Δ is the geocentric distance in meters, $hc\nu$ is the energy (J) of a photon with wavenumber ν (cm^{-1}), $f(x)$ is the fraction of molecules expected in the sampled region (see appendix of Hoban et al., 1991), and F_i is the flux (W m^{-2}) from line i incident on the terrestrial atmosphere. The photodissociation lifetime (τ) is taken to be 1.32×10^5 s for CH_4 (Huebner et al., 1992), and g_i is the line fluorescence efficiency (photons s^{-1} molecule^{-1}), both of which are calculated for a heliocentric distance of 1 AU. Our Q-curves increase with distance from the nucleus due to seeing, comet drift, and other observing factors, until a terminal value is reached, which we take to be the "global" production rate. The ratio between the terminal production rate and the nucleus-centered value is typically 3–4 for CSHELL observations and 1.5–2.5 for NIRSPEC observations. This methodology is used to analyze all our molecular emissions, including the OH^* quadruplet discussed below. Example Q-curves for both NIRSPEC and CSHELL data are shown in Fig. 2. The NIRSPEC Q-curves (Lee on August 21 and A2 on 10 July) combine both the R0 and R1 lines to improve signal-to-noise. When using this method, the derived production rates are less sensitive to seeing, drift of the comet perpendicular to the slit, and potential optical depth effects.

Opacity effects were evaluated following the methodology outlined in DiSanti et al. (2001) for calculating the critical radius (R_c) at which $\tau = 1$ at line-center. We find that CH_4 optical depth effects are not important for any comet in this paper. The worst case scenarios are for Hyakutake on UT 24 March due to its close proximity to Earth and Hale–Bopp on 24 February owing to the high production rate. We calculate $R_c < 0.2$ and 4 km (corresponding to 0.003 and 0.004 arcsec) for R0 in Hyakutake and Hale–Bopp, respectively. This is well within the central 0.2-arcsec pixel for each comet.

3. A fluorescence model for CH_4

Methane is a symmetric tetrahedral hydrocarbon. It lacks a permanent dipole moment and hence has no pure rotational lines and cannot be observed at radio wavelengths. It also does not fluoresce efficiently at visible or UV wavelengths. Determination of CH_4 production rates in comets is therefore dependent on observations of ro-vibrational transitions in the infrared. The strongest of these is the ν_3 band near

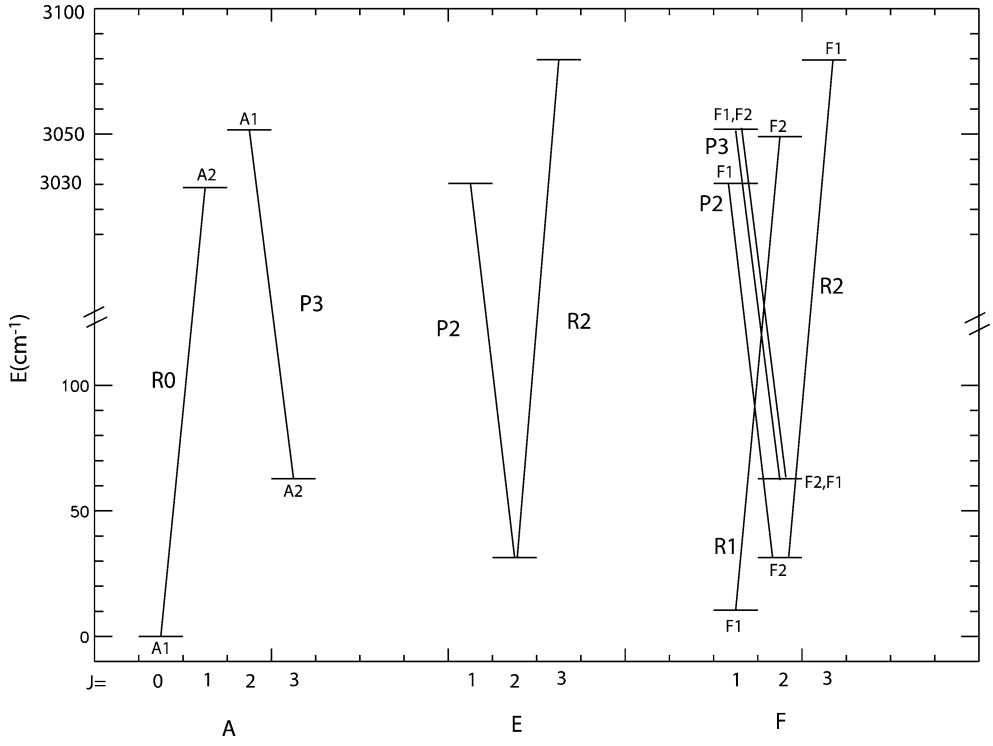

Fig. 3. An energy level diagram for methane showing the R0, R1, R2, P2, and P3 transitions for all three spin states.

3.3 μm. To analyze our data, we need to know the fluorescence efficiency (g-factor) of each observed methane transition for a wide range of rotational temperatures appropriate to cometary comae. These are expected to range from less than 50 to 150 K (or perhaps higher). Toward this end, we developed a fluorescence emission model for the methane ν_3 band.

The CH_4 molecule has three non-combining spin species labeled A, E, and F with equilibrium statistical weights of 5, 2, and 3, respectively. The A and F spin species are comprised of A_1, A_2 and F_1, F_2, respectively. The only transitions allowed under electric-dipole selection rules are $A_1 \leftrightarrow A_2$, $E \leftrightarrow E$, and $F_1 \leftrightarrow F_2$ with selection rules $\Delta J = 0$, ± 1 and $\Delta R = 0$ (where R is the rotational angular momentum). Figure 3 shows an energy level diagram for the R0, R1, R2, P2, and P3 lines. The A, E, and F ladders are shown separately.

Our CH_4 model calculates g-factors by assuming that the lower state rotational populations are in local thermodynamic equilibrium at a rotational temperature ($T_{\rm rot}$):

$$n = \omega_j \exp(-hc\nu/kT)/Z(T), \tag{2}$$

where ω_J is the statistical weight and Z is the partition function at temperature $T = T_{\rm rot}$. The rotational partition functions for each spin species are given in Fox (1970). The g-factor is determined (at $R_h = 1$ AU) using

$$g_{\rm lu} = \rho_\odot B_{\rm lu} n, \tag{3}$$

where $\rho_\odot$ is the solar flux at 1 AU (3.306×10^{13} photons $\mathrm{cm}^{-2}\,\mathrm{s}^{-1}\,(\mathrm{cm}^{-1})^{-1}$ near 3.3 μm based on a solar brightness temperature of 5760 K) and $B_{\rm lu}$ is the Einstein absorption coefficient given by

$$B_{\rm lu} = S_{\rm line}(T)/f(T), \tag{4}$$

where $S_{\rm line}$ is the line strength and f is the fractional population in the $v = 0$ rotational level at T. The temperature-independent g-factor for the ν_3 band is determined to be 3.54×10^{-4} photons $\mathrm{molecule}^{-1}\,\mathrm{s}^{-1}$. This excludes contributions from possible cascade into the ν_3 level from higher lying vibrational states (e.g., $\nu_3 + \nu_4 - \nu_3$). The line strengths at 296 K are taken from the HITRAN database (McClatchey et al., 1973; Rothman et al., 1998). The resulting g-factors for select lines and rotational temperatures appropriate for comet observations (50–150 K) are given in Table 2. Because we cannot resolve the blended spin states in our observations of the P2 line, it is treated as a single line having the sum of the appropriate g-factors.

We do not observe enough lines to adequately sample the distribution of rotational populations, and so we are not able to derive accurate rotational temperatures for CH_4. While up to four lines were observed in two comets (R0, R1, P2, P3 in Hyakutake and Lee), the observations were taken at different times and with different grating settings. Hence, they are subject to calibration uncertainties and possible variations in cometary activity, both of which hinder rotational analysis. The R0 and R1 lines, observed simultaneously with NIRSPEC, have a small difference in lower state energy (Table 2), hence the ratio of their intensities is not very sensitive to rotational temperature for values of $T_{\rm rot}$ expected in the coma. The P3 line is blended with emission from the

Table 2
CH_4 ν_3 g-factors

Transition	ν_0 (cm^{-1})	E_l[a] (cm^{-1})	g-factors*				
			50 K	75 K	100 K	125 K	150 K
R0 (A1-A2)	3028.752	0.00	4.316	2.383	1.557	1.118	0.8525
R1 (F1-F2)	3038.499	10.48	3.153	1.925	1.322	0.9787	0.7615
R2 (F2-F1)	3048.153	31.44	2.444	1.824	1.386	1.090	0.8827
(E-E)	3048.169		1.629	1.216	0.9240	0.7264	0.5884
P2 (F2-F1)	2998.994	31.44	0.9797	0.7312	0.5556	0.4367	0.3537
(E-E)	2999.060		0.6524	0.4869	0.3700	0.2908	0.2356
P3 (A2-A1)	2988.795	62.88	1.080	1.090	0.9627	0.8285	0.7127
(F2-F1)	2988.932		0.6518	0.6564	0.5795	0.4984	0.4287
(F1-F2)	2989.033		0.6513	0.6570	0.5804	0.4995	0.4297
P4 (F2-F1)	2978.650	104.78	0.2713	0.4055	0.4366	0.4232	0.3942
(E-E)	2978.848		0.1801	0.2705	0.2918	0.2831	0.2639
(F1-F2)	2978.920		0.2697	0.4057	0.4377	0.4247	0.3959
(A1-A2)	2979.012		0.4470	0.6742	0.7282	0.7069	0.6591

* In units of 10^{-5} photons $molecule^{-1}$ s^{-1}.
[a] Lower state energy.

CH_3OH ν_2 band. However, the degree of contamination by CH_3OH cannot be determined since there exists no satisfactory low-temperature fluorescence model for this band of methanol. For this reason, P3 is not used in our analysis. We therefore adopt rotational temperatures derived from analysis of CO, HCN, and H_2O. It is unknown whether collisions will equilibrate T_{rot} in CH_4 with that found for other molecules. However, analyses of relative Q-branch intensities for the ν_7 band (Dello Russo et al., 2001) of C_2H_6 (also an apolar molecule) are consistent with T_{rot} found for these molecules, suggesting that this is a reasonable assumption. Further, our analysis of molecules having a wide range of dipole moments indicates that T_{rot} is not sensitive to the degree of molecular polarity (e.g., CO and HCN can typically be characterized by a similar T_{rot} even though their dipole moments differ by a factor of nearly 30). The derived rotational temperatures range from $\sim$ 50 to 150 K for the Oort cloud comets in our sample.

We also investigated the effect of varying spin temperature in our model. R0 and R1 sample different spin species (A and F, respectively), and the ratio of their intensities is dependent on both rotational temperature and spin temperature. Figure 4 shows the ratio of the F and A spin states as a function of T_{spin}. The uncertainty in T_{rot} for each comet is typically about 10 K (Table 3). This results in 10 and 20% uncertainties in the predicted intensity ratios for R0 and R1 for temperatures of 150 and 50 K, respectively. Including the stochastic noise and calibration uncertainties (for CSHELL only), our total uncertainty is typically 20–30%. When we analyze the R0 and R1 lines separately, we find the ratios of line intensities to be consistent with statistical equilibrium to within 1-σ. According to Fig. 4, this corresponds to $T_{spin} > 40$ K. However, a 1-σ uncertainty of 10% in R1/R0 is consistent with a spin temperature greater than $\sim$ 30 K, and a 20% uncertainty is consistent with a spin temperature greater than $\sim$ 25 K. More methane lines need to be observed and rotational temperatures better constrained before the spin temperature of methane in comets can be established definitively.

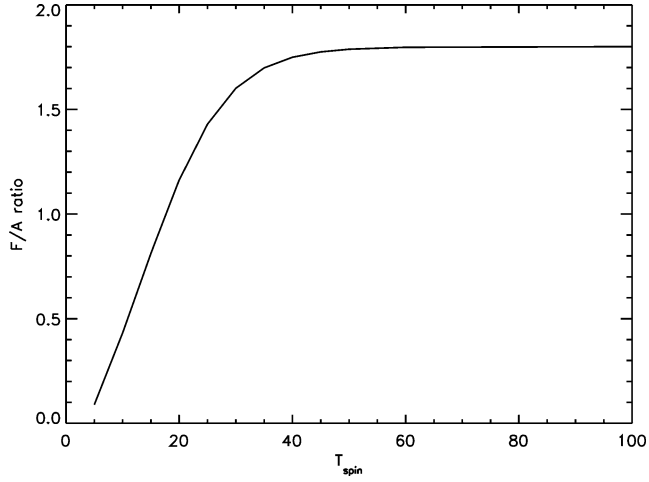

Fig. 4. The relative populations of F and A spin states (F/A) are shown as a function of T_{spin}.

4. Methane in comets

Our production rates for CH_4 are reported in Table 3, along with the rotational temperatures used to calculate them. The 1-σ uncertainties in Q(CH_4) Table 3 include stochastic error and uncertainties in rotational temperature as discussed above. CSHELL observations include an additional 10% uncertainty in flux calibration. Relative abundances obtained with NIRSPEC are better constrained since methane and water were observed simultaneously, eliminating calibration uncertainties. In a few cases, the calibration

Table 3
CH_4 mixing ratios

Comet	Date (UT)	Line	T_{rot}[a]	Flux[h]	Aperture (arcsec)	$Q(CH_4)$[b] ($\times 10^{26}$)	$Q(H_2O)$[a] ($\times 10^{28}$)	CO/H_2O[c] (%)	CH_4/CO	CH_4/H_2O (%)
Hyakutake	24.4 March 1996	R0 *(East)*	60(5)	86.1 (2.3)	2–8	38.6(7.1) *20.2(4.4)*	25.4(2.5)	17.3(2.0)	0.08(0.01) *0.04(0.01)*	**1.52(0.32)** ***0.80(0.19)***[d]
		R1 *(East)*		56.2 (3.7)	2–8	32.7(6.2) *18.4(3.8)*				**1.29(0.28)** ***0.72(0.16)***[d]
	10.2 April 1996	P2[f]	90(10)	8.86 (0.81)	2–8	34.5(6.7)	41.7(4.2)	13.9(2.5)	0.06(0.01)	**0.83(0.18)**
	12.2 April 1996	R0	100(10)	10.9 (0.56)	2–8	29.2(5.5)	39.9(7.6)	15.7(3.2)	0.05(0.01)	**0.73(0.20)**
		R1		10.6 (0.82)	2–8	32.2(6.0)				**0.81(0.22)**
		P2[f]		13.0 (0.84)	2–8	47.9(9.9)				**1.20(0.36)**
Hale–Bopp	24.2 February 1997	R0	90(10)	61.4 (1.3)	2–8	837(153)	889(89)	9.9(1.0)	0.09(0.02)	**0.94(0.20)**[e]
	30.0 April 1997	R0	90(10)	70.1 (0.76)	2–8	1048(189)	676(33)	14.4(0.8)	0.10(0.01)	**1.55(0.29)**
		R1		50.7 (4.8)	2–8	879(186)				**1.30(0.28)**
	1.0 May 1997	R0	90(10)	76.7 (2.9)	2–8	1118(202)	743(41)	12.9(0.8)	0.12(0.02)	**1.50(0.28)**
Lee	19.6 August 1999	R0 + R1	75(10)	3.02 (0.94)	0.5–3.5	18.4(4.2)	11.6(1.2)	2.0(0.3)	0.8(0.2)	**1.59(0.25)**
	21.6 August 1999	R0 + R1	75(10)	2.66 (0.09)	0.5–3.5	16.2(3.2)	12.6(1.0) *13(1)*[*]	1.8(0.2)	0.7(0.1)	**1.29(0.27)**[g]
S4	13.6 July 2000	R0 + R1	70	0.50 (0.09)	0.5–3.5	1.0(0.3)	5.53(0.6)	0.45(0.34)	0.5(0.4)	**0.18(0.06)**
McNaught–Hartley	4.7 March 2001	R0	50(10)	1.3 (0.3)	2–5	8.1(3.0)	5.7(2.4)	∼ 17	∼ 0.08	**1.4(0.8)**
A2	9.5 July 2001	R0 + R1	85(10)	1.97 (0.15)	0.5–3.5	3.23(0.65)	3.11(0.24) *3.1(0.4)*[*]			**1.04(0.22)**
	10.5 July 2001	R0 + R1	85(10)	2.99 (0.24)	0.5–3.5	5.15(0.99)	3.46(0.34) *3.2(0.4)*[*]	∼ 4 *∼ 0.7*[FUSE]		**1.49(0.32)**
WM_1	23.3 November 2001	R0 + R1	50[i]	0.62 (0.03)	0.5–3.5	0.86(0.17)	*2.5(0.3)*[*]			**0.34(0.08)**
Ikeya–Zhang	21.9 March 2002	R0	140(10)	8.7 (1.1)	2–8	36.3(5.8)	66(5)	∼ 4.7	0.12	**0.55(0.10)**
		R1		7.4 (0.7)	2–8	35.0(8.5)				**0.53(0.13)**
	22.9 March 2002	R1	140(10)	9.5 (0.8)	2–8	43.9(7.5)	95(13)			**0.46(0.10)**

Note: Our production rates are determined from mean emission intensities on either side of the nucleus measured in 1-arcsec intervals over the aperture indicated above. This information can be obtained in tabular form by contacting ELG.

[*] From OH lines.

[a] References for $Q(H_2O)$ and T_{rot}: Hyakutake (Dello Russo et al., 2002); Hale–Bopp (Dello Russo et al., 2000); Lee (Mumma et al., 2001b); S4 (Mumma et al., 2001a); Ikeya–Zhang (Dello Russo et al., 2003); WM_1 water production rates are from the OH^* quadruplet; A2 values are from OH^* quadruplet and (Dello Russo et al., in preparation); McNaught–Hartley (Mumma et al., 2001c; DiSanti et al., in preparation).

[b] 15% was added to CSHELL data to compensate for emission outside the 5 column extract.

[c] References for native CO/H_2O: Hyakutake (DiSanti et al., 2003); Hale–Bopp (DiSanti et al., 2001); Lee (Mumma et al., 2001b); S4 (Mumma et al., 2001a); McNaught–Hartley (Mumma et al., 2001c); A2 (Feldman et al., 2002) (FUSE), (DiSanti et al., in preparation); Ikeya–Zhang (DiSanti et al., 2002); WM_1 is still under analysis but preliminary reductions indicate that this comet is depleted in CO (DiSanti et al., in preparation).

[d] Due to apparent short-term asymmetry west of the nucleus during the time of the CH_4 observations, the production rate of CH_4 may be artificially enhanced with respect to water. The lower production rate (in italics) is found by generating a Q curve only on the points east of the nucleus.

[e] The water production rate on 24.2 February is significantly higher than predicted by the water production evolution curve derived in Dello Russo et al. (2000). If the heliocentric fit value for Q_{H_2O} is used, then $Q_{CH_4}/Q_{H_2O} = 1.23 \pm 0.26\%$.

[f] The P2 line has 2 unresolved components. The atmospheric transmittance was found at the Doppler shifted position of each component to be the same within 2%. In this case we used an average transmittance and summed the g-factors of the two components to derive a production rate.

[g] This value is significantly different from the 0.8% previously reported in Mumma et al. (2001b), due primarily to an improved atmospheric model fit for the methane lines. Also, the assumed g-factor was 13% larger than that determined by our current model.

[h] Total transmittance corrected line flux (10^{-18} W m^{-2}) in the aperture indicated and centered on the peak of the CH_4 emission.

[i] Assumed.

star may not have been centered in the slit or the seeing was poor during a stellar observation. Both effects can increase uncertainties associated with correcting for slit losses. In these cases, the calibration from another night on the same observing run was used.

Whenever possible, water production rates were obtained from H_2O spectral lines measured directly near 5, 2.9, and 2 μm. These non-resonant fluorescent transitions are excited from the ground vibrational level by optical pumping and they terminate on states that are only sparsely populated (and hence are only weakly absorbing) in the terrestrial atmosphere. Their physics is well understood, and we routinely use them to determine water production rates in comets (e.g., Mumma et al., 1996; Dello Russo et al., 2001).

We also inferred water production rates from prompt emission in the OH^* quadruplet near 3045 cm^{-1} (these lines fall in the same spectral order as the CH_4 R0 and R1 lines, see Fig. 1). This OH* quadruplet is a set of high J ($v' = 1$, $J' = 11.5$ and 12.5) lines that result from dissociation of water by UV photolysis. Once produced, they promptly emit at infrared wavelengths. The resulting P-branch emission forms a set of quadruplets in a wide range of rotational states spanning much of the L-band. Their spatial profile tracks that of the parent (H_2O, see Fig. 5). Hence, they should provide a good proxy for the water production rate. The effective g-factor for this multiplet of OH^* was inferred in comet Lee to be 2×10^{-7} molecules s^{-1} at $R_h = 1$ AU (Mumma et al., 2001b). We assume this value to be the same in other comets, independent of the H_2O rotational temperature. When available, both values for the water production rate are quoted, and they are usually found to be in agreement (see Table 3).

C/1996 B2 (Hyakutake)

We report detections of CH_4 in Hyakutake with CSHELL on three dates in 1996. On 24.4 March and 12.2 April, strong emissions due to both the R0 and R1 lines were detected. Additionally, the P2 line was observed on 10.2 and 12.2 April. The April dates are consistent with 0.8% CH_4 (all abundances are given with respect to water unless otherwise noted).

From Table 3, it might be inferred that Hyakutake varied significantly between the March and April observations, with the mixing ratio in March nearly twice that found in April. We note, however, the presence of an asymmetric outflow during the earlier observations on 24.4 March (Dello Russo et al., 2002; DiSanti et al., 2003). This can be seen in the bottom panel of Fig. 5, which shows the spatial profile of the CH_4 R0 line (solid line) compared to that of the dust emission (dashed line). The R0 profile is extended to the west, but it matches the eastern component of the dust profile. In contrast, the spatial profile of methane in Lee (top panel, solid line) matches that of the dust (dashed line), which is what we typically see in comets. We also typically find that the CH_4 spatial profile matches those of other native species such as water and C_2H_6, both of which are consistent with release solely from the nucleus for all comets in our database (Dello Russo et al., 2002).

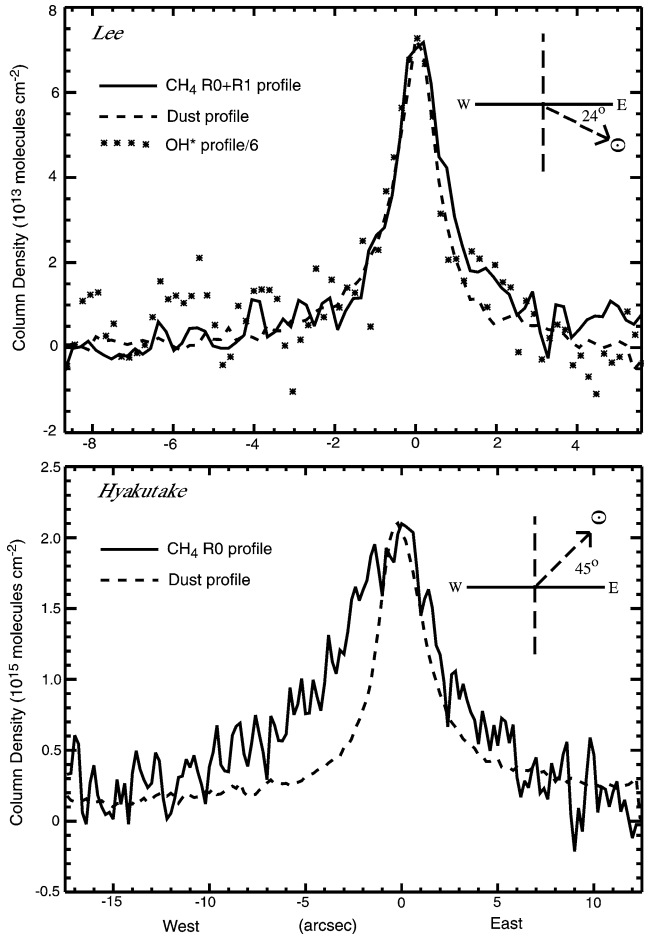

Fig. 5. Spatial profiles of dust (dashed line) and CH_4 (solid line) emission in comet Lee (combined R0 and R1 lines) on 21.6 August, 1999 (top) and Hyakutake (R0 line only) on 24.4 March, 1996 (bottom). Also shown is the OH prompt emission ($*$) profile in Lee which matches the profiles for native gases like CH_4. This is typically the case. CH_4 in Hyakutake shows substantial excess in emission west of the nucleus-centered position, possibly indicating the presence of a short-term jet phenomenon at the time of the observation (see text).

We suspect this behavior may be related to the proximity of Hyakutake to Earth (0.106 AU) in late March 1996 as well as its rapid rotation. At this distance, and assuming an outflow velocity of ~ 800 m s^{-1}, material leaving the nucleus can traverse the length of the slit in less than 25 minutes. By the time water was observed (> 75 minutes after the CH_4 R1 line and > 35 minutes after the CH_4 R0 line), the gas emission profile more closely matched that of the dust, with just a minor enhancement to the west. A short-term westward increase in activity could explain the apparent enhancement. Rotation of a jet out of the field of view could also explain the differences in the CH_4 profile relative to those observed later in the day (Dello Russo et al., 2002). This behavior is not inconsistent with the fast rotation period in March (6.23 hours) determined by Schleicher et al. (1998). Assuming this rotation period, the comet will have rotated > 72

degrees and > 34 degrees between the CH_4 R1 and R0 exposures, respectively, and the first water exposure. Thus a column containing an enhanced number of molecules (e.g., a jet) could have rotated out of the slit in the time between the methane and water exposures. DiSanti et al. (2003) also discuss evidence for variations in CO on this date.

If the production rate for CH_4 is determined only from the points east of the nucleus, the mixing ratio is found to be in agreement with the April dates. Since the enhanced mixing ratio in March (in the east-west mean) could possibly be explained by a jet or a short-term enhancement in activity that is not apparent in the later water exposures, we can neither prove nor disprove the existence of heterogeneity in the methane mixing ratio in Hyakutake based on the 24.4 March observations. A detailed analysis of the 24.4 March data set, which is beyond the scope of this paper, would be required to answer these questions. This illustrates that one must be cautious when interpreting mixing ratios for molecules that are not observed simultaneously, as is often the case for CSHELL observations. Water and CH_4 are observed simultaneously with NIRSPEC, alleviating such uncertainties.

C/1995 O1 (Hale–Bopp)

CH_4 was observed in Hale–Bopp on 24.2 February, 30.0 April and 1.0 May 1997. The R0 line was observed on all dates and the R1 line only on 30.0 April. The 24.2 February data result in a lower mixing ratio, but the water production rate was significantly higher than predicted by the heliocentric fit to $Q(H_2O)$ in Dello Russo et al. (2000). Magee-Sauer et al. (1999) also noted a lower mixing ratio for HCN on this date if the observed production rate for water was used. If the heliocentric fit value for Q_{H_2O} is used, then $Q_{CH_4}/Q_{H_2O} = 1.23 \pm 0.26\%$, consistent with that determined from the April and May observation. Hale–Bopp was one of the comets most enriched in CH_4, in addition to being very rich in CO (DiSanti et al., 2001).

C/1999 H1 (Lee)

Results for R0 and R1 are reported for two dates (19.6 and 21.6 August 1999) in comet Lee, the first comet observed with NIRSPEC. We determine a mixing ratio of $\sim 1.45\%$, which makes Lee, along with Hale–Bopp, the richest CH_4 comets (we note that this value is significantly higher than that reported in Mumma et al. (2001b), see note to Table 3). Lee is also notable for having the highest CH_4/CO ratio observed to date, more than double that determined for any other comet in our data set, due to its combination of depleted CO and abundant CH_4.

C/1999 S4 (LINEAR)

S4 was observed with NIRSPEC on one night (13.6 July 2000) prior to its complete disruption later that month. Both the R0 and R1 lines are clearly visible (Fig. 1), though quite weak when compared to the other comets. This comet had the lowest CH_4/H_2O ratio of any other Oort cloud comet observed to date and was found to be depleted in other volatiles as well (Mumma et al., 2001a), consistent with a warmer formation temperature, perhaps in the Jupiter/Saturn region of the protoplanetary disk.

C/1999 T1 (McNaught–Hartley)

A single line of R0 was detected in McNaught–Hartley using CSHELL on 4.7 March 2001. The water production rate for 13 January 2001 was reported by Mumma et al. (2001c), along with a CH_4 upper limit of 1.6%. Preliminary water production rates for 4/5 March ($5.7(2.4) \times 10^{28}$ molecules s^{-1}, DiSanti et al., in preparation) are consistent with what is derived by assuming an insolation limited heliocentric dependence ($\sim 5 \times 10^{28}$ molecules s^{-1}) based on the 13 January water production rate. Both the direct and extrapolated values for $Q(H_2O)$ result in a mixing ratio of $\sim 1.5(0.8)\%$. While the signal-to-noise (~ 6) of the R0 line is somewhat low, McNaught–Hartley is likely not a low methane (< 0.5%) comet.

C/2001 A2 (LINEAR)

A2, observed on 9.5 and 10.5 July 2001, exhibited several outbursts associated with major disruptions of the nucleus prior to our observations (Mattiazzo et al., 2001; Seargent et al., 2001; Hergenrother et al., 2001). This presented an opportunity to potentially investigate the composition of freshly exposed material from the interior of a comet nucleus. The mixing ratios, while suggestive of an increase between these two dates, are consistent to within the 1-σ uncertainty. A CO production rate of $\sim 1.3 \times 10^{27}$ molecules s^{-1} was reported by Feldman et al. (2002) for 12 July 2001 using the Far Ultraviolet Spectroscopic Explorer (FUSE). Their value is consistent with our preliminary CO production rate, though their water production rate ($2 \pm 1 \times 10^{29}$ s^{-1}) does not agree with the values we obtain from either the OH^* quadruplet (this work) or from H_2O hot band emission (Dello Russo et al., in preparation; see Table 3). They determine $Q(CO)/Q(H_2O) \approx 0.7\%$ (compared to the $\sim 4\%$ determined from our preliminary analysis). It must be pointed out that the FUSE observations occurred during an outburst, and it is possible that the mixing ratio for CO changed between the two observations. Nonetheless, CO appears to be somewhat depleted in A2 (< 4%), while no such depletion in CH_4 is observed.

C/2000 WM_1 (LINEAR)

WM_1 was a dynamically new comet for which we report CH_4 detections on 23.3 November 2001. We assume $T_{rot} = 50$ K, consistent with preliminary data analysis. WM_1 appears to be somewhat depleted in CH_4, though not to the extent of comet S4, and preliminary analysis indicates that this comet is also depleted in CO (DiSanti et al., in preparation).

153/P Ikeya–Zhang (C/2002 C1)

Comet Ikeya–Zhang was, at its brightest, available for daytime observing with CSHELL. CH_4 was measured on

two dates in March 2002 during exceptional observing conditions. The R1 line was detected on both 21.9 and 22.9 March. The R0 line was observed on 21 March. Ikeya–Zhang was somewhat depleted, with about 0.5% CH_4, or $\sim$ 10% the abundance of CO. Other volatiles were in the range typically found for most comets (DiSanti et al., 2002; Dello Russo et al., 2002; Magee-Sauer et al., 2002). This comet was also observed with the Infrared Camera and Spectrograph (IRCS) at Subaru by Kawakita et al. (2003) on 28.3 and 29.3 May using similar observing and reduction protocols. While they did not measure water, their CH_4/C_2H_6 ratio is consistent with ours (~ 0.82).

4.1. Discussion: methane in Oort cloud comets

It is immediately obvious from Table 3 that the abundance of CH_4 relative to water varies among our sample of comets, with extreme mixing ratios differing by nearly an order of magnitude. This is graphically evident in Fig. 6, which shows the CH_4 R1 line and two of the OH* quadruplet lines, corrected for geocentric Doppler shift, in a sample of three comets: Lee (21.6 August), WM_1 (23.3 November), and S4 (13.6 July). Each spectrum was corrected for atmospheric transmittance at the Doppler-shifted line-center frequencies and was scaled to bring the integrated intensity over its OH^* lines to a common value. Since these three comets exhibit comparable rotational temperatures (for CO, HCN, H_2O, and C_2H_6), this difference in relative CH_4 line intensities probably represents true variations in mixing ratios. The weakest CH_4 R1 line is in comet S4, which is depleted in all measured organic species (Mumma et al., 2001a). WM_1 and Ikeya–Zhang are also somewhat depleted in CH_4, though not to the extent of S4. Hale–Bopp, Hyakutake, A2, McNaught–Hartley and Lee all seem to have CH_4 abundances in the range $\sim$ 0.8–1.5% relative to water. These are consistent with abundances seen in icy grain mantles in massive star forming regions (Boogert et al., 1996).

One noticeable trend can be seen in the CH_4/H_2O mixing ratio among comets. Figure 7 shows a weighted average of mixing ratios in comets based on the data in Table 3. On dates with unusual circumstances (24.4 March 1996 for Hyakutake and 24.2 February 1997 for Hale–Bopp), not all data were averaged. The Hyakutake average is calculated using the April dates and only the eastern emission on 24.4 March since these data exhibit an unusual westward enhancement (discussed above). Only the April data were used for the Hale–Bopp average since the apparently enhanced water production rate on 24.2 February resulted in lower mixing ratios for many species (Dello Russo et al., 2000; Magee-Sauer et al., 1999).

It is apparent from Fig. 7 that our data do not show a clear-cut boundary between "methane-poor" and "methane-rich" comets. These results suggest a fairly continuous distribution of mixing ratios for methane among Oort cloud comets observed to date. This differs from most other molecules observed at infrared wavelengths. Ethane, for example, has a mixing ratio of about 0.6–0.7% reported for most comets observed to date, with S4 and A2 being the only exceptions so far (Dello Russo et al., 2001, 2002). Native CO in this same sample of comets is found to be $\leqslant 5\%$ in some comets and $> 10\%$ in others (DiSanti et al., 2001, 2002; Mumma et al., 2001a, 2001b, 2001c), with an apparent absence of intermediate CO mixing ratios. HCN varies by a factor of four among the comets observed so far, but is found to be around 0.2% relative to water for the majority of them (Magee-Sauer et al., 2001, 2002 and references therein; Mumma

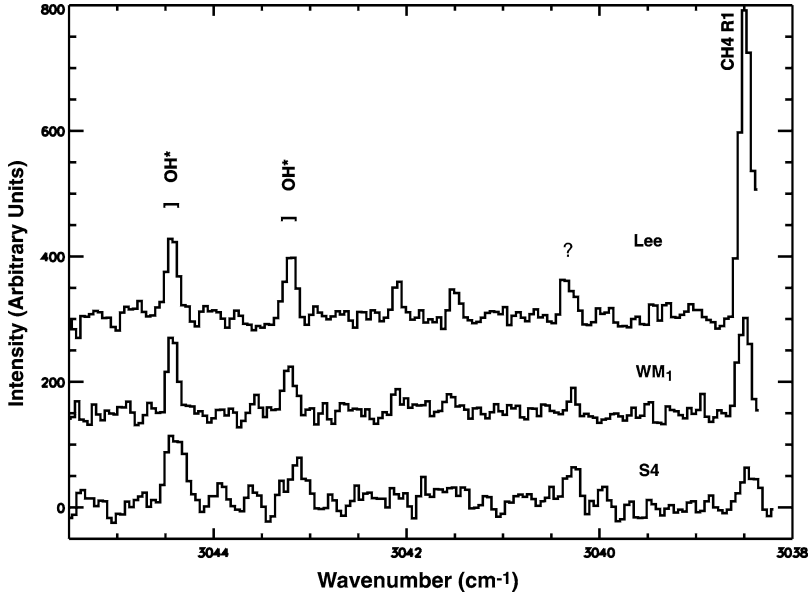

Fig. 6. Plot showing the relative intensities of the R1 CH_4 line to OH prompt emission (OH^*) in comets Lee (top), WM_1 (middle), and S4 (bottom). The spectra have been shifted to the comet's rest frequency, corrected for atmospheric transmittance, and scaled to bring the integrated intensity over the OH^* lines (representing water, see text) to a common value. This shows that there are substantial variations in CH_4/H_2O ratio among our sample of comets.

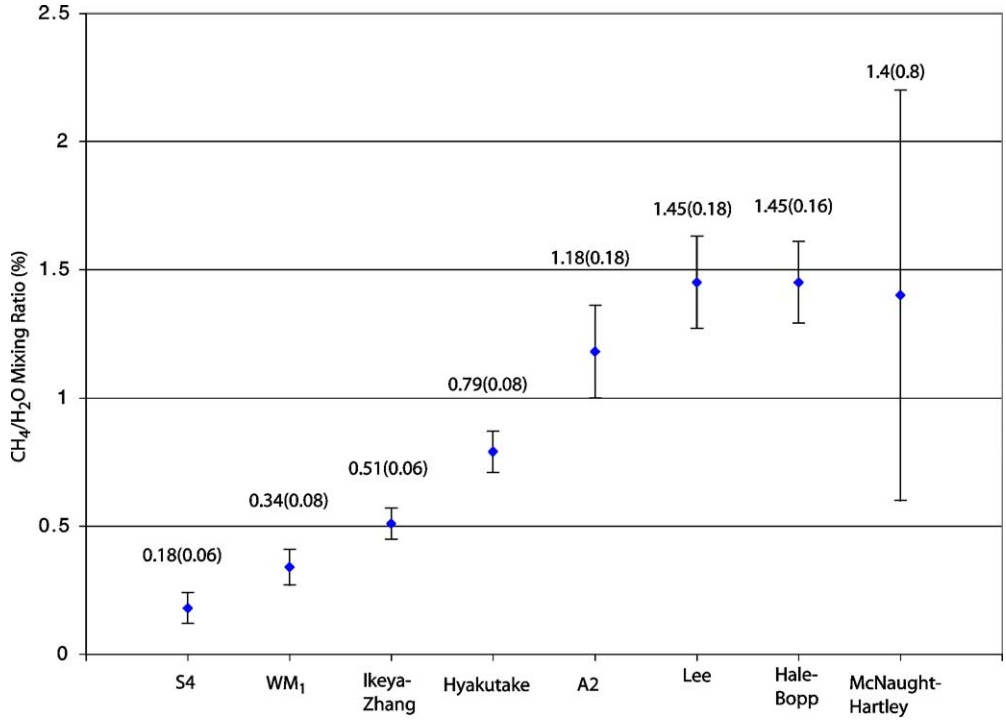

Fig. 7. The mixing ratio of CH_4/H_2O in all eight Oort cloud comets. For comets observed multiple times, the values shown are a weighted average of the mixing ratios in Table 3. Only the April data were used for Hale–Bopp and the western emission component was omitted in the March dates for Hyakutake, as discussed in Section 4.

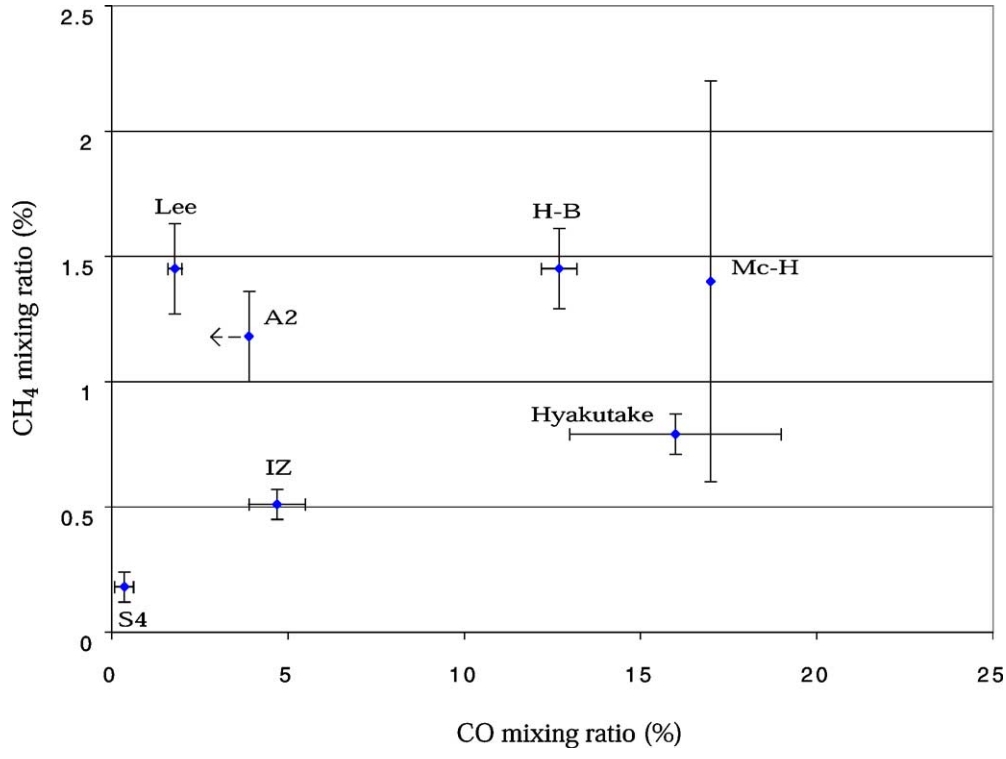

Fig. 8. A plot of CH_4 vs. CO mixing ratios. The figure shows that the two hypervolatiles do not appear to be correlated. While comets depleted in CH_4 ($< 0.5\%$) have not been observed to be rich in CO ($> 10\%$), comets with 0.5–1.5% CH_4 comprise both the low- and high-CO comets. Of particular interest is comet Lee with nearly the same mixing ratio for both CO and CH_4, whereas the CH_4/CO ratio is < 0.3 for the remaining comets in our data set. A possible exception is A2 where FUSE results give 0.7% CO (~ 5 times lower than our preliminary reductions, hence the arrow on the plot indicating that CO mixing ratio is less than $\sim 4\%$). Clearly A2 is not among the CO-rich comets. Uncertainties in the CO mixing ratio for McNaught–Hartley have not been reported.

et al., 2001b). Our results reveal significant variations in CH_4/H_2O among Oort cloud comets, and they demonstrate that measurements of many more comets are required before general statements concerning trends in parent volatile abundances among the OC population can be discerned.

4.2. Heterogeneity

One unanswered question in cometary science is the extent to which a cometary nucleus is heterogeneous. Radial transport mechanisms within the protoplanetary disk could have resulted in cometesimals that formed at different radii sticking together to form a single comet, giving a body comprised of smaller units of varying composition. We have multiple observations of many comets taken at different times, but we do not, within the uncertainty, see conclusive evidence of heterogeneity in the data presented here. The differences seen in A2 between 9.5 and 10.5 July are suggestive of such heterogeneity (Gibb et al., in preparation).

5. Interstellar and nebular comparisons

It has been suggested that if temperature alone controlled the composition of pre-cometary ices, then the two comparably hypervolatile species CH_4 and CO (sublimating at 31 and 24 K, respectively; Crovisier and Encrenaz, 2000) should be correlated. It is immediately apparent from Table 3 and Fig. 8 that the mixing ratios for native CO and CH_4 show no apparent correlation. While no comets depleted in CH_4 ($< 0.5\%$) have yet been observed to have high CO ($> 10\%$) mixing ratios, comets with 0.5–1.5% CH_4 comprise both the low and high CO comets. This result is surprising if the ice mantles coating pre-cometary grains accreted at a specific temperature in the protoplanetary disk since both CH_4 and CO would be expected to condense under similar conditions. This would argue against temperature as the dominant factor, at least in determining the abundances of hypervolatiles in comets. To explain the observed composition, we must therefore explore other options.

What does determine the hypervolatile abundance of a comet? That may depend on the extent to which pre-cometary grains retained their icy mantles, on mechanisms of gas-phase production and destruction, and on details of trapping or recondensing of gas onto grain surfaces. Radial transport mechanisms within the disk may have played an important role as well. It must also be kept in mind that the chemistry and physics of the protoplanetary nebula were time dependent. Cometary composition may depend on "when" as well as "where" a comet formed.

Desorption may occur initially via shock heating of infalling interstellar grains upon impact with the gas of the protoplanetary disk. The degree to which the grain is heated depends on the density of material it is impacting and hence on the radial distance from the young Sun. According to current models, dust infalling beyond ~ 30 AU may have entered the protoplanetary disk gently enough to retain most of the polar ice mantle (Neufeld and Hollenbach, 1994; Chick and Cassen, 1997) while grains inward of 30 AU would have lost their volatiles.

Once within the protoplanetary disk, grains were subject to viscous heating, which would have been more severe closer to the young Sun. For grains within ~ 10 AU, the temperatures during the time of comet formation may have been too warm to condense hypervolatiles such as CO and CH_4. On the other hand, temperatures beyond 100 AU may never have exceeded 20 K or so (Boss, 1998), permitting most of the interstellar volatile ice mantle to be retained.

In the interstellar medium, the C–H ν_4 deformation mode of solid CH_4 on icy grain mantles has been observed at 7.67 μm in the envelopes of young stellar objects (YSOs; Boogert et al., 1996). The position and width of the ice feature is consistent with the presence of CH_4 in a polar (H_2O-rich) matrix, but not in the apolar (CO-rich) ice. This is consistent with formation of CH_4 via hydrogen atom addition to atomic C on the surface of the grain, analogous to the formation route for H_2O. Further evidence for CH_4 being formed by H-atom addition in a polar matrix is the fact that CH_4 gas in star-forming regions, unlike the CO gas, is not observed to have a cold component consistent with its low (~ 31 K) sublimation temperature. This is consistent with evaporation at the high ($\geqslant 100$ K) temperatures found in the hot cores of star forming regions (Boogert et al., 1998). Thus, CH_4 could have survived in grain mantles at much higher temperatures than those implied by its 31 K evaporation temperature. If the polar mantle was completely evaporated in warmer regions, retained in regions where the temperature never exceeded ~ 100 K, and partially evaporated in intermediate regions, this could have led to distance dependent variability of solid (and gaseous) CH_4 in the young disk.

Transport mechanisms are also thought to have played a significant role in the chemistry of the protoplanetary disk. Some grains must have been exposed to high temperatures, as evidenced by the discovery of crystalline silicates in comets (Campins and Ryan, 1989; Hanner et al., 1997). Such grains would have lost their original ice mantles and accreted new ones from the gas phase after turbulent mixing transported them to a region where temperatures were sufficiently low. The analyses of Wooden et al. (1999), Colangeli et al. (1999), and Crovisier et al. (2000) suggest that crystalline silicates were a significant (in some cases dominant) contributor to the total silicate inventory of Hale–Bopp. This implies efficient outward turbulent mixing of material from the inner nebula (Bockelée-Morvan, 2002). Likewise, viscosity-driven radial migration may have taken material rich in ice from the outer disk (beyond 100 AU) and transported it inward. If the temperatures of these grains remained low, a significant fraction of pristine interstellar material may have been retained. Hence, there may have been substantial mixing of methane-rich and methane-poor grains through much of the giant-planet region.

In addition to thermal and transport considerations, there are also models for methods of formation or destruction of CH_4 in the nebula. It has been proposed that a possible formation route for methane was through Fischer–Tropsch catalysis between 1 and 5 AU (Kress and Tielens, 2001) or by carbon dust oxidation in the inner disk near 0.5 AU (Gail, 2002). If turbulent mixing was as efficient as implied by interpretations of crystalline silicates in Hale–Bopp (Bockelée-Morvan, 2002), then any CH_4 that formed in the inner nebula could also have been transported to cometary formation distances.

As the disk cooled, volatile constituents may have been trapped in the form of clathrate hydrates. Iro et al. (2003) suggest that all CH_4 would be easily trapped throughout the giant-planet region. This scenario could explain the observed variability in CO but does not explain the observed variability in CH_4. However, while in the gas phase, CH_4 could have undergone destructive ion-molecule reactions (Aikawa et al., 1999), and these could have significantly altered its abundance as a function of radial distance from the young Sun in the re-condensed ice.

It would seem that low-methane (and low-CO) comets are consistent with formation at warm temperatures (like those expected near the Jupiter/Saturn region) where a small CH_4 (and CO) component may exist in a polar mantle, either by retention of original interstellar material or by trapping in clathrate hydrates. In the case of dynamically new comets, depletion of methane may also be due in part to surface modification by cosmic rays during their extensive residency in the Oort cloud (Strazzulla and Baratta, 1992), assuming of course that the processed layer is not lost prior to the observation. Comets that formed in cooler regions may have retained some interstellar CH_4 ice and could be further influenced by transport within the disk and any gas phase production/destruction routes.

The different physical and chemical processes discussed above could help explain the variations in CH_4 seen among the comets observed to date. While not a comprehensive list, this discussion serves to give a general idea of the conditions that may have influenced the volatile content of cometary ices. Clearly, advances in modeling and a greater database of observations are needed to fully explain the complex picture of comet formation that is emerging.

6. Summary

We report abundances of CH_4 in eight Oort cloud comets based on our high-dispersion infrared spectra and our model for fluorescent emission in the ν_3 band near 3.3 μm. Methane mixing ratios vary among these comets, with nearly an order of magnitude separating the most depleted and richest sources observed to date. The results of this study indicate a fairly continuous distribution of methane among Oort cloud comets ranging from ~ 0.15–1.5%. It will be interesting to see if this trend survives as CH_4 abundances are measured for more comets. We also find the R0 and R1 line intensities to be consistent with statistical equilibrium, although spin temperatures of 25–30 K cannot be excluded at this point. CH_4 clearly does not correlate with CO in our sample of Oort cloud comets, which seems to indicate that temperature was not the dominant factor in controlling the hypervolatile composition of comets.

Multiple observations of a comet on different dates may be used to test for heterogeneity within the nucleus. We see no definitive evidence of heterogeneity in CH_4 based on the data presented in this paper.

Too little is known of the actual physical conditions in protoplanetary disks to accurately predict comet abundances. However, it is clear that temperature, ion-molecule reactions, radial migration, or grain-surface reactions alone are insufficient to explain observations and that more detailed model calculations and observations of disks are needed to understand the complex network of conditions under which comets formed. With each new comet observed, more interesting and unusual discoveries are being made about comet taxonomy, and we are adding to our understanding of the processes and conditions in the early solar nebula.

Acknowledgments

E.L. Gibb gratefully acknowledges support from the National Research Council under her Resident Research Associateship. This work was also supported by NASA Planetary Astronomy RTOP 693-344-32-30-07 to M.J. Mumma. N. Dello Russo was supported by NASA Planetary Atmospheres program grants NAG5-10795 and NAG5-12285. M.A. DiSanti was supported by NASA Planetary Astronomy program grants NAG5-7905 and NAG5-12208. K. Magee-Sauer was supported by the National Science Foundation Research at Undergraduates Institution program under grant AST-009841. We give a special thank you to H. Weaver for collaborating on WM_1 observations at the W.M. Keck Observatory. We also acknowledge vital assistance provided by staffs of the IRTF and Keck in acquiring the data. The W.M. Keck Observatory is operated as a scientific partnership among the California Institute of Technology, the University of California and the National Aeronautics and Space Administration. The Observatory was made possible by the generous financial support of the W.M. Keck Foundation. The NASA IRTF is operated by the University of Hawaii under contract to NASA. The authors recognize and acknowledge the very significant cultural role and reverence that the summit of Mauna Kea has always had within the indigenous Hawaiian community. We are most fortunate to have the opportunity to conduct observations from this mountain.

References

Aikawa, Y., Umebayashi, T., Nakano, T., Miyama, S.M., 1999. Evolution of molecular abundances in proto-planetary disks with accretion flow. Astrophys. J. 519, 705–725.

Biver, N., Bockelée-Morvan, D., Colom, P., Crovisier, J., Germain, B., Lellouch, E., Davies, J.K., Moreno, R., Paubert, G., Wink, J., Despois, D., Lis, D.C., Mehringer, D., Benford, D., Gardner, M., Phillips, T.G., Gunnarsson, M., Winnberg, A., Bergman, P., Johansson, L.E.B., Rauer, H., 1999. Long-term evolution of the outgassing of Comet Hale–Bopp from radio observations. Earth Moon Planets 78, 5–11.

Bockelée-Morvan, D., Gautier, D., Hersant, F., Hur, J.-M., Robert, F., 2002. Turbulent radial mixing in the solar nebula as the source of crystalline silicates in comets. Astron. Astrophys. 384, 1107–1118.

Boogert, A.C.A., Schutte, W.A., Tielens, A.G.G.M., Whittet, D.C.B., Helmich, F.P., Ehrenfreund, P., Wesselius, P.R., de Graauw, Th., Prusti, T., 1996. Solid methane toward deeply embedded protostars. Astron. Astrophys. 315, L377–L380.

Boogert, A.C.A., Helmich, F.P., van Dishoeck, E.F., Schutte, W.A., Tielens, A.G.G.M., Whittet, D.C.B., 1998. The gas/solid methane abundance ratio toward deeply embedded protostars. Astron. Astrophys. 336, 352–358.

Boss, A.P., 1998. Temperatures in protoplanetary disks. Annu. Rev. Earth Planet. Sci. 26, 53–80.

Brooke, T.Y., Tokunaga, A.T., Weaver, H.A., Chin, G., Geballe, T.R., 1991. A sensitive upper limit on the methane abundance in Comet Levy (1990c). Astrophys. J. 372, L113–L116.

Campins, H., Ryan, E.V., 1989. The identification of crystalline olivine in cometary silicates. Astrophys. J. 341, 1059–1066.

Chick, K.M., Cassen, P., 1997. Thermal processing of interstellar dust grains in the primitive solar environment. Astrophys. J. 477, 398–409.

Colangeli, L., Brucato, J.R., Ferrini, L., Mennella, V., Bussoletti, E., Palumbo, P., Rotundi, A., 1999. Analysis of cosmic materials: results on carbon and silicate laboratory analogues. Adv. Space Res. 23, 1243–1252.

Crovisier, J., 11 colleagues, 2000. The thermal infrared spectra of Comets Hale–Bopp and 103P/Hartley 2 observed with the infrared space observatory. In: Sitko, M.L., Sprague, A.L., Lynch, D.K. (Eds.), Thermal Emission Spectroscopy and Analysis of Dust Disks, and Regoliths. In: Astron. Soc. Pac. Conf. Ser., Vol. 196, p. 109.

Crovisier, J., Encrenaz, T., 2000. Comet Science. Cambridge Univ. Press, Cambridge, UK.

Dello Russo, N., DiSanti, M.A., Mumma, M.J., Magee-Sauer, K., Rettig, T.W., 1998. Carbonyl sulfide in Comets C/1996 B2 (Hyakutake) and C/1995 O1 (Hale–Bopp): evidence for an extended source in Hale–Bopp. Icarus 135, 377–388.

Dello Russo, N., Mumma, M.J., DiSanti, M.A., Magee-Sauer, K., Novak, R., Rettig, T.W., 2000. Water production and release in Comet C/1995 O1 Hale–Bopp. Icarus 143, 324–337.

Dello Russo, N., Mumma, M.J., DiSanti, M.A., Magee-Sauer, K., Novak, B., 2001. Ethane production and release in Comet C/1995 O1 Hale–Bopp. Icarus 153, 162–179.

Dello Russo, N., Mumma, M.J., DiSanti, M.A., Magee-Sauer, K., 2002. Production of ethane and water in Comet C/1996 B2 Hyakutake. J. Geophys. Res.-Planet. 107 (E11), 5095. 10.1029/2001JE001838.

Dello Russo, N., DiSanti, M.A., Magee-Sauer, K., Gibb, E.L., Mumma, M.J., 2003. Water production and release in Comet 153P/Ikeya–Zhang (C/2002 C1): accurate rotational temperature retrievals from hot-band lines near 2.9 μm. Icarus. Submitted.

DiSanti, M.A., Mumma, M.J., Dello Russo, N., Magee-Sauer, K., Novak, R., Rettig, T.W., 2001. Spatially resolved carbon monoxide emission in comet Hale–Bopp: production rates and rotational temperatures vs. heliocentric distance. Icarus 153, 361–390.

DiSanti, M.A., Dello Russo, N., Magee-Sauer, K., Gibb, E.L., Reuter, D.C., Mumma, M.J., 2002. CO, H_2CO, and CH_3OH in Comet 2002 C1 Ikeya–Zhang. In: The Proceedings for the Asteroids, Comets, Meteors Conference, Berlin, Germany, 2002. In: ESA SP, Vol. 500, pp. 571–574.

DiSanti, M.A., Mumma, M.J., Dello Russo, N., Magee-Sauer, K., Griep, D.M., 2003. Evidence for a dominant native source of carbon monoxide in Comet C/1996 B2 (Hyakutake). J. Geophys. Res.-Planet. In press.

Drapatz, S., Larson, H.P., Davis, D.S., 1987. Search for methane in Comet P/Halley. Astron. Astrophys. 187, 497–501.

Feldman, P.D., Weaver, H.A., Burgh, E.B., 2002. Far ultraviolet spectroscopic explorer observations of CO and H_2 emission in Comet C/2001 A2 (LINEAR). Astrophys. J. 576, L91–L94.

Fox, K., 1970. On the rotational partition function for tetrahedral molecules. J. Quant. Spectrosc. Radiat. Transfer 10, 1335–1342.

Gail, H.-P., 2002. Radial mixing in protoplanetary accretion disks III. Carbon dust oxidation and abundance of hydrocarbons in comets. Astron. Astrophys. 390, 253–265.

Hanner, M.S., Gehrz, R.D., Harker, D.E., Hayward, T.L., Lynch, D.K., Mason, C.C., Russel, R.W., Williams, D.M., Wooden, D.H., Woodward, C.E., 1997. Thermal emission from the dust coma of Comet Hale–Bopp and the composition of the silicate grains. Earth Moon Planets 79, 247–264.

Hergenrother, C.W., Chamberlain, M., Chamberlain, Y., 2001. Comet C/2001 A2 (LINEAR). IAU Circ. 7616.

Hoban, S., Mumma, M.J., Reuter, D.C., DiSanti, M., Joyce, R.R., 1991. A tentative identification of methanol as the progenitor of the 3.52-μm emission feature in several comets. Icarus 93, 122–134.

Huebner, W.F., Keady, J.J., Lyon, S.P., 1992. Solar photo rates for planetary atmospheres and atmospheric pollutants—photo rate coefficients and excess energies. Astrophys. Space Sci. 195, 7.

Iro, N., Gautier, D., Hersant, F., Bockelee-Morvan, D., Lunine, J.I., 2003. An interpretation of the nitrogen deficiency in comets. Icarus 161, 511–532.

Kawakita, H., Watanabe, J., Kinoshita, D., Ishiguro, M., Nakamura, R., 2003. Saturated hydrocarbons in Comet 153P/Ikeya–Zhang: ethane, methane, and monodeuterio–methane. Astrophys. J. 590, 573–578.

Kawara, K., Gregory, B., Yamamoto, T., Shibai, H., 1988. Infrared spectroscopic observation of methane in Comet P/Halley. Astron. Astrophys. 207, 174–181.

Kress, M.E., Tielens, A.G.G.M., 2001. The role of Fischer–Tropsch catalysis in solar nebula chemistry. Meteorit. Planet. Sci. 36, 75–91.

Kunde, V.G., Maguire, J.C., 1974. Direct integration transmittance model. J. Quant. Spectrosc. Radiat. Transfer 14, 803–817.

Larson, H.P., Weaver, H.A., Mumma, M.J., Drapatz, S., 1989. Airborne infrared spectroscopy of Comet Wilson (1986I) and comparisons with Comet Halley. Astrophys. J. 338, 1106–1114.

Magee-Sauer, K., Mumma, M.J., DiSanti, M.A., Dello Russo, N., Rettig, T.W., 1999. Infrared spectroscopy of the ν_3 band of hydrogen cyanide in C/1995 O1 Hale–Bopp. Icarus 142, 498–508.

Magee-Sauer, K., Mumma, M.J., DiSanti, M.A., Dello Russo, N., 2001. Infrared observations of HCN and C_2H_2 in five Oort-cloud comets. Bull. Am. Astron. Soc. 33, 2009.

Magee-Sauer, K., Dello Russo, N., DiSanti, M.A., Gibb, E.L., Mumma, M.J., 2002. Production of HCN and C_2H_2 in Comet C/2002 C1 Ikeya–Zhang on UT April 13.8 2002. In: The Proceedings for the Asteroids, Comets, Meteors Conference, Berlin, Germany, 2002. In: ESA SP, Vol. 500, pp. 549–552.

Mattiazzo, M., Bouma, R.J., Raymundo, P.M., Linnolt, M., Amorim, A., Nagai, Y., Ree, S.T., Cernis, K., 2001. Comet C/2001 A2 (LINEAR). IAU Circ. 7605.

McClatchey, R.A., Benedict, W.S., Clough, S.A., Burch, D.E., Calfee, R.F., Fox, K., Rothman, L.S., Garing, J.S., 1973. AFCRL. TR-73-0096. Environmental Research Papers, No. 434.

Mumma, M.J., DiSanti, M.A., Dello Russo, N., Fomenkova, M., Magee-Sauer, K., Kaminski, C.D., Xie, D.X., 1996. Detection of abundant ethane and methane, along with carbon monoxide and water, in Comet C/1996 B2 Hyakutake: evidence for interstellar origin. Science 272, 1310–1314.

Mumma, M.J., Dello Russo, N., DiSanti, M.A., Magee-Sauer, K., Novak, R.E., Brittain, S., Rettig, T., McLean, I.S., Reuter, D.C., Xu, L.H., 2001a. The startling organic composition of C/1999 S4 (LINEAR): a comet formed near Jupiter? Science 292, 1334–1339.

Mumma, M.J., McLean, I.S., DiSanti, M.A., Larkin, J.E., Dello Russo, N., Magee-Sauer, K., Becklin, E.E., Bida, T., Chaffee, F., Conrad, A.R., Figer, D.F., Gilbert, A.M., Graham, J.R., Levenson, N.A., Novak, R.E., Reuter, D.C., Teplitz, H.I., Wilcox, M.K., Xu, L.H., 2001b. A survey of

organic volatile species in Comet C/1999 H1 (Lee) using NIRSPEC at the Keck Observatory. Astrophys. J. 546, 1183–1193.

Mumma, M.J., Dello Russo, N., DiSanti, M.A., 2001c. Comet C/1999 T1 (McNaught–Hartley). IAU Circ. 7578.

Neufeld, D.A., Hollenbach, D.J., 1994. Dense molecular shocks and accretion onto protostellar disks. Astrophys. J. 428, 170–185.

Roche, A.E., Wells, W.C., Cosmovici, C.B., Drapatz, S., Michel, K.W., 1975. An upper limit for methane production from Comet Kohoutek by high resolution tilting-filter photometry at 3.3-micron. Icarus 24, 120–127.

Rothman, L.S., Rinsland, C.P., Goldman, A., Massie, S.T., Edwards, D.P., Flaud, J.-M., Perrin, A., Camy-Peyret, C., Dana, V., Mandin, J.-Y., Schroeder, J., McCann, A., Gamache, R.R., Wattson, R.B., Yoshino, K., Chance, K., Jucks, K., Brown, L.R., Nemtchinov, V., Varanasi, P., 1998. The HITRAN molecular spectroscopic database and HAWKS (HITRAN Atmospheric Workstation). 1996 edition. J. Quant. Spectrosc. Radiat. Transfer 60, 665–710.

Schleicher, D.G., Millis, R.L., Osip, D.J., Leder, S.M., 1998. Activity and the rotation period of Comet Hyakutake (1996 B2). Icarus 131, 233–244.

Seargent, D.A.J., Baransky, A., Hasubick, W., Morris, C.S., 2001. Comet C/2001 A2 (LINEAR). IAU Circ. 7611.

Strazzulla, G., Baratta, G.A., 1992. Carbonaceous material by ion irradiation in space. Astron. Astrophys. 266, 434–438.

Wooden, D.H., Harker, D.E., Woodward, C.E., Butner, H.M., Koike, C., Witteborn, F.C., McMurtry, C.W., 1999. Silicate mineralogy of the dust in the inner coma of Comet C/1995 01 (Hale–Bopp) pre- and postperihelion. Astrophys. J. 517, 1034–1058.